# Chemical Kinetic Modeling in Coal Gasification Processes: an Overview

Slavinskaya N.A.[1*], Riedel U.[1], Messerle V.E.[2], Ustimenko A.B.[2]

[1]Institute of Combustion Technology German Aerospace Center (DLR),
Stuttgart, Germany
[2]Research Institute of Experimental and Theoretical Physics, Al-Farabi Kazakn National University,
Almaty, Kazakhstan

## Abstract

Coal is the fuel most able to cover world deficiencies in oil and natural gas. This motivates the development of new and more effective technologies for coal conversion into other fuels. Such technologies are focused on coal gasification with production of syngas or gaseous hydrocarbon fuels, as well as on direct coal liquefaction with production of liquid fuels. The benefits of plasma application in these technologies is based on the high selectivity of the plasma chemical processes, the high efficiency of conversion of different types of coal including those of low quality, relative simplicity of the process control, and significant reduction in the production of ashes, sulphur, and nitrogen oxides. In the coal gasifier, two-phase turbulent flow is coupled with heating and evaporation of coal particles, devolatilization of volatile material, the char combustion (heterogeneous/porous oxidation) or gasification, the gas phase reaction/oxidation (homogeneous oxidation) of gaseous products from coal particles. The present work reviews literature data concerning reaction kinetic modelling in coal gasification. Current state of related kinetic models for heterogeneous/homogeneous oxidation of coal particles, included plasma assisted, is reviewed.

## Introduction

The new electric power (electricity) generation concepts, such as co-firing or combined gasification gas turbines (IGCC plant) help reduce the dependency on fossil fuels and decrease $CO_2$ emissions. Gasification (partial combustion, reforming) is the cleanest, most flexible and reliable way of utilizing fossil fuels. It can convert waste into high-value products, such as substitute natural gas, transport fuels, etc. New, more effective coal gasification technologies are required in order to ensure the highest acceptable range in the variation of fuel composition and conditions and therefore a higher efficiency of the process. Plasma-assisted gasification can be considered one of possibilities to accelerate and optimize coal gasification [1, 2]. Its main advantages are high selectivity, possibility to produce different types of materials and of full automation, reduced emissions of $CO_2$, nitrogen and sulfur oxides and soot. The study of coal gasification applying thermal and non-equilibrium plasma was started at the beginning of the 1960's. Extensive, mostly experimental data has been collected which allows to determine the main properties of the processes and develop a number of acetylene and syngas production units. Considerably less research is devoted to detailed modelling of chemical and physical processes of plasma-assisted gasification. In coal gasifier, two-phase turbulent flow is accompanied by heating and evaporation of coal particles, devolatilization of volatile material, combustion of char (heterogeneous/porous oxidation) or gasification, the gas phase reaction/oxidation (homogeneous oxidation) of gaseous products from coal particles. The present work reviews literature data concerning reaction kinetic models used in coal gasification modeling.

### *Physico-Chemical Processes in Gasifiers*

Chemical structure and composition of coal are dependent on coal rank or metamorphism. That is determined with age of coal and can be presented with such sequence: lignum fossile (peat) < brown (pitch) coal < flame coal (candelit) < gas-flame coal < gas-coal < fat coal < smithing coal < green (lean) coal < anthracite coal. Generally, coal is a 3D polymer with non-regular structure but with repeating frag-

* Corresponding author. E-mail: nadja.slavinskaya@dlr.de

ments, which can be selected as "coal molecules" [3, 4], see Fig. 1. These are composed of an aromatic centre and aliphatic periphery. Main atoms in such molecules are C, H, O, S, N. In dependence of type, place of digging, etc. coal can contain the different inclusions mostly $H_2O$, Si, Al, Fe, Ca, Mg, Ti, different tars, etc. The weight of "coal molecules", the content of atoms C and number of saturated aromatic rings in it increase with coal rank. The number of H and O atoms decreases with age of coal [4].

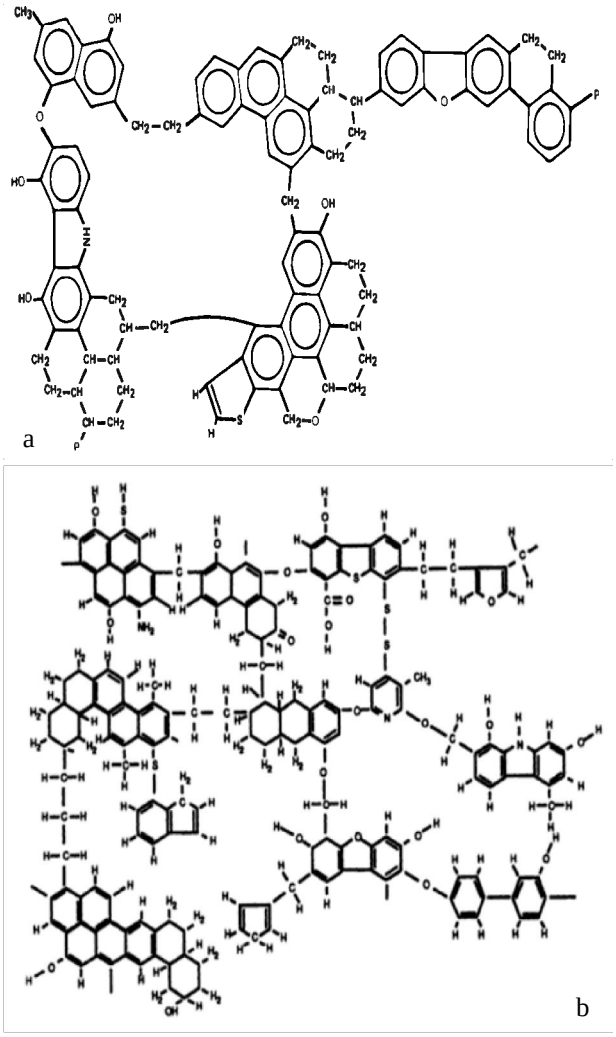

Fig. 1. Models of "coal molecules" [3].

Coal gasification, Fig. 2 [5], is conducted through particle heating accompanied by evaporation of volatile material and coal pyrolysis; heterogeneous/porous reactions between coal particle and gas phase environment; chemical reactions in the gas phase (homogeneous oxidation) between gaseous products from coal gasification/oxidation; mostly heterogeneous reaction of char, produced from coal particles during devolatilization, with gaseous products. The main gaseous products in gasifier are $O_2$, CO, $CO_2$, $H_2O$, $H_2$ and $CH_4$. All described processes are accompanied by two-phase turbulent flow. A complete description of coal gasification is not possible, due to the complexity of physical and chemical processes interacting. However, based on experiments and simplified chemical mechanisms, this process can be divided into several sub-models, which can be studied separately. Chemical modelling becomes even more complicated in plasma-assisted coal gasification. The processes, which can be affected by plasma, are shown in Fig. 2.

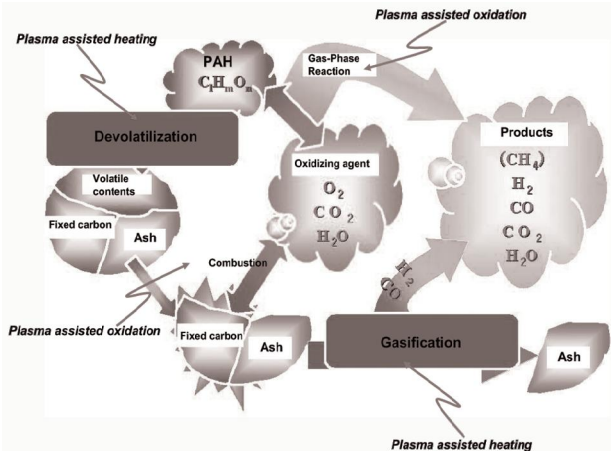


Fig. 2. Principal scheme of physical and chemical processes by coal gasification to be modeled (used design of [5]).

Coal reactivity is affected by different variables: coal rank, thermal history of the char (pyrolysis), pore structure, chemical structure of coal, reactive gases concentration, pressure, sample size [6-14]. The interplay among the transport and chemical reaction mechanisms determines whether burning rates are governed by the chemical kinetics, internal pore diffusion, or external film diffusion [10]. Under typical pulverized fuel (p.f.) firing conditions, this intrinsic formulation quickly shifts from chemical kinetics regime during the ignition stage to the external film diffusion regime during quasi-steady combustion at the hottest particle temperatures. As the particle burns, the core of remaining combustible material shrinks, so the burning regime can shift back into chemical kinetics controlling regime, in which $O_2$ completely penetrates the internal pore structure and both external film and intraparticle diffusion resistances are negligible [10].

Processes of coal devolatilization and gasification of carbon have been discussed widely in the literature for many years. Different CFD tools were developed to model the turbulent flow in different types of coal gasifiers: KIVA COAL & KIVA II numerical approach [15] for modeling of devolatiliza-

tion of coal particles, char and volatile combustion; MBED-1 [16] proved one-dimensional model for countercurrent oxidation and gasification of coal in fixed or slowly moving beds. The model incorporates an advanced devolatilization sub-model that can predict the evolution rates and the yields of individual gas species and tar; Cinar ICE Code [17] was designed to provide computational solutions of industrial problems, especially those related to two-phase combustion; G. Liu et al. [18] developed an approach to predict a particle structure parameter used in the random pore model; L. Yang [7] mathematical models on the underground coal gasification are established according to their storage conditions and features of gas production process; TERRA [19] is the computation of multi-component heterogeneous systems with own database of thermo-chemical properties for > 3.500 chemical agents over a temperature interval 300-6000 K; Piffaretti S. et al. [20] proposed CFD model for aerodynamics within the boiler based on chemical processes described with EDM – Eddy Dissipation Model, PPDF – Presumed Probability Density Function Model, EDM + PPDF – rate determined as the slower of the two models, Fig. 3; in project [5] for coal gasification numerical code FLUENT with RESORT (Revolutionary Software Orchestrated Reactions in Turbulent Flow) application was used. An entrained-flow gasification CFD simulators are capable to analyse flow, reaction, and heat transmission at the same time calculate temperature, particle rate distribution, ash adhesion locations, gas composition, etc. within a gasifier if given as input data such parameters as reactor shapes, operation conditions, coal property and reaction data. Carbon Burnout Kinetics (CBK) is a kinetics package that describes char conversion under conditions relevant to pulverized fuel processes. It was developed by Prof. Robert Hurt both at Sandia National Laboratories, Livermore, and currently, at Brown University [9, 10]. The version CBK/E [9] is specially designed for carbon burnout applications, treats the stages of char combustion in detail, includes all the same transport-related and annealing mechanisms, including single-film char combustion, intraparticle reaction/diffusion, thermal annealing, and ash inhibition. The further expanded version of CBK for char gasification is called CBK/G [10]. It predicts the rate of gasification, the char particle temperature, and the changes in the particle diameter and density as gasification proceeds, given a gas temperature, radiative exchange temperature, and partial pressures of the gasification agents.

Computer models for coal gasification design require easily integrated numerical sub-models, which describe the chemical processes inside and outside particles, in surrounding gas phase and also interaction between heterogeneous and homogeneous chemistry. At present it is not possible to model the entire process using all fundamental steps, because of insufficient kinetic data. Sub-models mostly used include three reaction sets: reactions describing devolatilization of coal particle, heterogeneous reactions of char, and reactions in gas phase (not always). As the vapour mass flow of volatile products is rather intensive the heterogeneous reactions of coal particle with surrounding environment (air, $O_2$, $CO_2$, $H_2O$, $H_2$) can be assumed negligible. Mostly global reaction schemes (intrinsic kinetics, not influenced by transport processes), i.e. reaction mechanisms with minimal sets of intermediate species and with reaction steps, which can be a combination of several elementar chemical reactions, are used in all cited tools. The stoihiometric coefficients and parameters for reaction rates are empirical and derived from the coal gasification experiments.

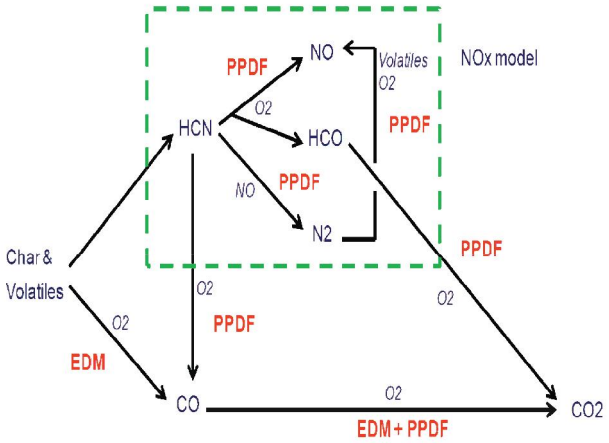


Fig. 3. Reaction pass model used in [20]. EDM – Eddy Dissipation Model, PPDF – Presumed Probability Density Function Model, EDM + PPDF – rate determined as the slower of the two models.

The analysis of most simple models of the char gasification (homogeneous models, and unreacted core models), which do not consider coal structural changes during process and any chemical reactions, can be found in [21]. These models do not distinguish the heterogeneous or homogenous reactions describing coal gasification with empirical overall reaction constants. They are preferred if the main intention for studying coal reactivity is just to describe the relation between time and conversion.

Simple global reaction sets of the carbon heterogeneous reactions can be found in [21-26]. The most common reactions used for coal gasification modeling are

$$C + CO_2 = 2CO$$
$$C + H_2O = CO + H_2$$
$$C + 2H_2O = CO_2 + 2H_2$$
$$C + 2H_2 = CH_4$$

The sub sets from 8 global reactions was used in [5] for simulation of devolatilization, heterogeneous and gas phase (heterogeneous) reactions, Table 1.

Reaction R1 has the first order, n = 1, the reaction order of R5 and reaction rates R1-R8 have been obtained from approximation of experimental data.

**Table 1**

Chemical sub-system used in [5].
FC-fixed carbon. VM-volatile molecule

| Devolatilization | |
|---|---|
| Coal →VM ($C_aH_bO_cN_dS_e$) + FC+ASH | R1 |
| Heterogeneous reactions (Char reactions) | |
| FC + 0.5 $O_2$ → CO | R2 |
| FC+ $CO_2$ → 2 CO | R3 |
| FC + $H_2O$ → CO + $H_2$ | R4 |
| Homogeneous reactions | |
| VM($C_aH_bO_cN_dS$) + $\rho O_2$ → $q$CO+$r$$H_2$+$s$$H_2$+$t$$H_2S$ | R5 |
| CO + 0.5 $O_2$ → $CO_2$ | R6 |
| $H_2$ + 0.5 $O_2$ → $H_2O$ | R7 |
| $C_3H_8$ + 5 $O_2$ → 3 $CO_2$ + 4 $H_2O$ | R8 |

The chemical scheme [27] used in numerical tool [19] for plasma assisted gasification, Table 2, consists of 51 chemical reactions and 25 chemical species, which developed to describe 3 different kinetic processes. The first 1-6 reactions describe the initialisation stage of coal conversion and devolatilisation. The second set, reactions 7-9 represent the carbon gasification and combustion.

Finally, the third sub mechanism contents the radical reactions of volatiles and gasification products with their further transformations. This model does not include specific plasma chemical reactions: the electric arc plasma was considered only as an internal heat source with a preset temperature profile.

In the work [13] the major features of kinetic models for low temperature coal oxidation are summarized. In [13] coal is assumed to oxidize at favoured sites on a pore's surface, that is, the co-called active sites. Two types of active site are assumed to responsible for the interaction between coal and oxygen molecules: type 1 for the active sites involved in burn-off reactions and type 2 for the sorption reaction sequence. Then, the direct burn-off reaction is written as:

$$C_{S1} + O_2 \rightarrow u_1CO_2 + v_1CO + w_1 \text{ other species}, k_1 \quad , \qquad (1)$$

where $C_{S1}$ is the concentration of active sites of type 1, parameters $u_1$, $v_1$ and $w_1$ are stoichiometric coefficients, which are necessary determined by experiment. Reaction (1) simplifies a few reaction steps, which may include rapid interaction between the active sites and $O_2$ and fast desorption of the gaseous products.

**Table 2**

Fragment of the reaction mechanism [27] used in [19]. Coefficient of reaction rate is $k_j = A_j*exp\ (-E/R*T)*T^{\beta}$, $R$ = 1,987*$10^{-3}$ (kcal*$mole^{-1}$*$degree^{-1}$), the units of preexponential factor $A_i$ are: for first order reactions ($n$ = *1*) - ($sec^{-1}$), for second order reactions – $n$ = *2* [$10^{-3}m^3$*$mole^{-1}$*$sec^{-1}$], activation energy $E_a$ – kcal*$mole^{-1}$

| # | LgA | $\beta$ | $E_A$ | Reaction |
|---|---|---|---|---|
| 1. | 18.20 | 0.0 | 88.8 | $H_{2T}=H_2$ |
| 2. | 13.90 | 0.0 | 51.4 | $H_2O_T=H_2O$ |
| 3. | 12.30 | 0.0 | 44.4 | $CO_T=CO$ |
| 4. | 11.30 | 0.0 | 32.6 | $CO_{2T}=CO_2$ |
| 5. | 14.20 | 0.0 | 51.6 | $CH_{4T}=CH_4$ |
| 6. | 11.90 | 0.0 | 37.4 | $C_6H_{6T}=C_6H_6$ |
| 7. | 5.20 | 0.0 | 29.0 | $C_T+H_2O=CO+H_2$ |
| 8. | 5.30 | 0.0 | 43.0 | $C_T+CO_2=CO+CO$ |
| 9. | 5.70 | 0.0 | 38.0 | $C_T+O_2=CO_2$ |
| 10. | 11.10 | 0.0 | 11.9 | $CH_4+H=CH_3+H_2$ |
| 11. | 5.00 | 3.08 | 2.0 | $CH_4+OH=CH_3+H_2O$ |
| 12. | 14.20 | 0.0 | 88.4 | $CH_4+M=CH_3+H+M$ |
| 13. | 10.20 | 0.0 | 9.2 | $CH_4+O=CH_3+OH$ |
| 14. | 9.80 | 0.0 | 24.8 | $CH_3+H_2O=CH_4+OH$ |
| 15. | 9.70 | 0.0 | 11.4 | $CH_3+H_2=CH_4+H$ |
| 16. | 13.30 | 0.0 | 91.6 | $CH_3+M=CH_2+H+M$ |
| 17. | 10.70 | 0.0 | 29.0 | $CH_3+O_2=CH_3O+O$ |
| 18. | 9.60 | 0.0 | 0.0 | $CH_3+OH=CH_2O+H_2$ |
| 19. | 11.10 | 0.0 | 2.0 | $CH_3+O=CH_2O+H$ |
| 20. | 10.70 | 0.0 | 21.0 | $CH_3O+M=CH_2O+H+M$ |

For further simplifications, the reactions in the adsorption sequence are reduced to the single overall step:

$$C_{S2} + O_2 \rightarrow u_2X_{P1} + v_2X_{P2} + w_2CO_2 + m \text{ in reactive compounds}, k \quad , \qquad (2)$$

where $X_{P1}$, $X_{P2}$ denote two types of oxygenated complex, that is, carboxyl and carbonyl species.

The reaction of thermal decomposition of the oxide complexes

$$X_{P1} \rightarrow CO_2 + \text{regenerated } C_{S2}, k_3 \qquad (3)$$
$$X_{P1} \rightarrow CO_2 + \text{regenerated d } C_{S2}, k_4 \qquad (4)$$

From (1)-(4) the rate expressions for the $O_2$ consumption and the production of carbon oxides can be determined. By fitting of these rate expressions to experimental data the coefficients of reaction rates, $k_1$, $k_2$, $k_3$, $k_4$, and stoichiometric coefficients for reactions (1)-(4) can be obtained.

The seven steps semi – global mechanism for char oxidation and gasification has been used in excellent studies [9, 10] at CBK modelling. This model is based on the work [12] and has such final reactions for steam and $CO_2$ gasification:

Combustion

$$2C + O_2 \rightarrow C(O) + CO \quad (5)$$

$$C + C(O) + O_2 \rightarrow C(O) + CO_2 \quad (6)$$

$$C(O) \rightarrow CO \quad (7)$$

Gasification

$$2C + CO_2 \rightarrow C(O) + CO \quad (8)$$

$$2C + O_2 \rightarrow C(O) + CO \quad (9)$$

$$C + H_2O \leftrightarrow C(O) + H_2 \quad (10)$$

$$C + 2H_2 \rightarrow CH_4 + H_2 \quad (11)$$

where C(O) denots the oxide complex on the carbon surface. Reactions (5) - (7) represent the burn-off and chemisorption reactions at the active sites, interaction of gaseous oxygen and surface oxygenated complex, and decomposition of the surface oxygenated complexes. The gasification reactions (8)-(11) are heterogeneous reactions of carbon with gas phase species $CO_2$, $O_2$, $H_2O$ and $H_2$ top form gas phase species and the oxide complexes. The gas phase reactions are not considered in [9, 10] – transport mechanism balances the consumption of reactant gases. Order of reactions, rate constants have been determined from analysis of experimental data for different stages of the coal gasification and from the fine tuning against the entire database. Applied assumption and simplification can be found in [9, 10].

The main problems of heterogeneous global modeling can be recognized in studies [9, 10, 12, 13]. More detailed kinetic models for the char combustion and gasification cam be found in [14, 28-30].

In work [28] in order to describe coal pyrolysis, in “coal molecules”, like shown on Fig. 1, were selected 10 functional groups HOH, O-O, OH, CO, COO, CHH, $CH_m$, $CH_z$, $CH_x$, and $CH_y$, which react with surrounding environment to produced CO, $CO_2$, $H_2$, $H_2O$, $CH_4$, $C_2H_6$, $(CH_z)_g$, tar and soot. Empirical parameters are used for reaction rates.

In [29] the entire course of carbon gasification, from 0 to 100% conversion, was simulated for the first time using molecular orbital theory, Fig. 4a. This method could simulate the following commonly observed features in actual gasification: (1) gasification starts at edge carbon atoms; (2) zigzag sites are more reactive than armchair sites; (3) specific rate increases monotonically with conversion. Furthermore, this simulation predicted that the specific rate depends on crystallite size, but is insensitive to crystallite shape.

Many authors [14, 30-36] consider the direct reactions between the active oxygen surfaces complexes and the gas phase molecules as the central point of the oxygen - char reaction. Chen et al. [30] suggested the more detailed main heterogeneous reaction paths with oxygenated complexes for oxygen, Fig. 4b, carbon dioxide, steam and hydrogen gasification. One of the most detailed reaction mechanisms for heterogeneous char oxidation with CO and $CO_2$ production is establish in [14]. In this work all free-surface active carbon sites is deviated in two groups: prisms-sites (Prismafläche), which lay on the boundary of single grapheme layer in the graphite structure, and basis sites (Basisfläche), which lay inside grapheme layer, Fig. 5.

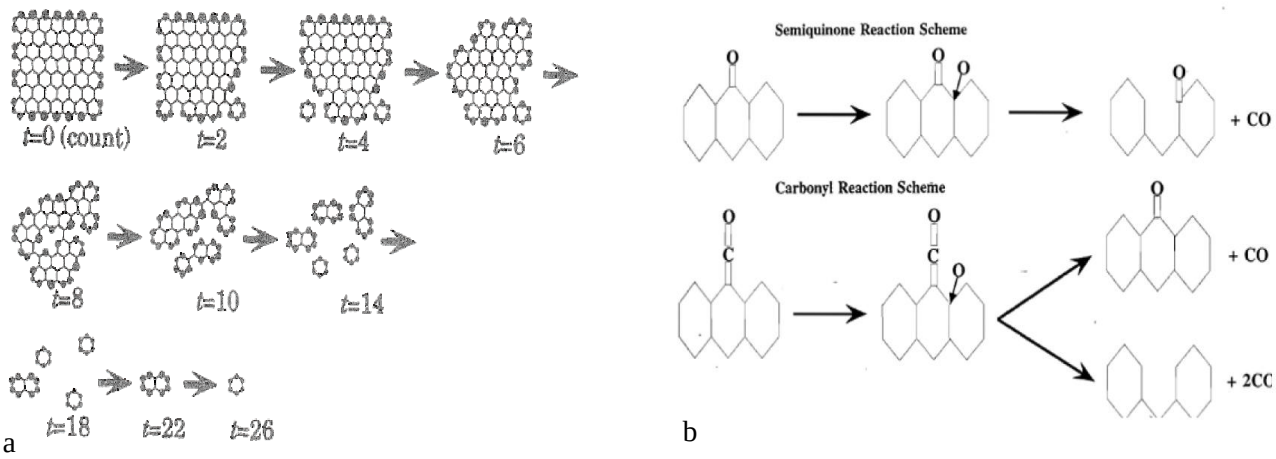


Fig. 4. Models of heterogeneous coal conversion: a) from [29] and b) from [30].

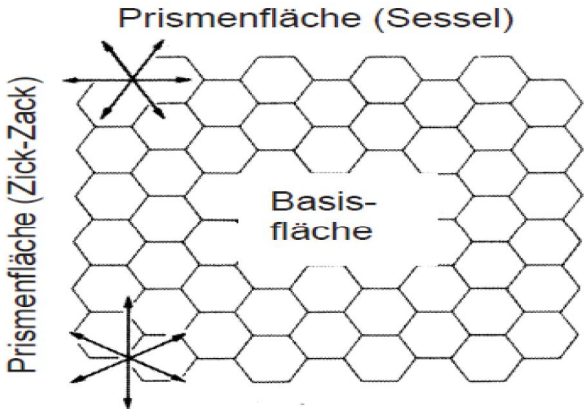

Fig. 5. Scheme of active sites used in [14].

To describe the basic mechanism (reaction with $O_2$) following surface complexes have been introduced in [14]:

- free-surface sites: prisms-sites (se), basis sites (sb)
- semiquinone O (se)
- carbonyl CO (se)
- lactone $CO_2$ (se)
- basis site complex O (sb)
- off-plane complex OT (s)
- intermediate species IOM (s)

A graphic representation of the surface complexes is shown on the Fig. 6. The detailed analysis of reaction mechanism developed for these complexes, Table 3, can be found in [14]. Last three reactions in Table 3 describe the gas phase reactions of produced CO. Reaction rates parameters have been obtained from literature experimental and theoretical data, where possible, or evaluated from thermo chemical properties. Main conclusion following from mechanism:

- dissociative chemisorption of $O_2$ takes place both at the prisms-sites and at the basis-sites of surface;
- gasification (the formation of carbon monoxide) applies only to prisms-sites;
- there is the surface diffusion of the adsorbed oxygen atoms from basis-sites to prisms sites on the particle surface;
- the chemisorption of oxygen on the basis-sites leads to the formation of off-plane complexes;
- the off-plane oxygen atoms weaknesses the adjacent C-C bonds.

Numerical simulations of the burnout rate and concentrations of CO and $CO_2$ performed with this mechanism are in good agreement with experimental data.

Mitchell at al. [37] has compiled an elementary adsorption-desorption surface reaction mechanism involving 16 species in 18 elementary reactions.

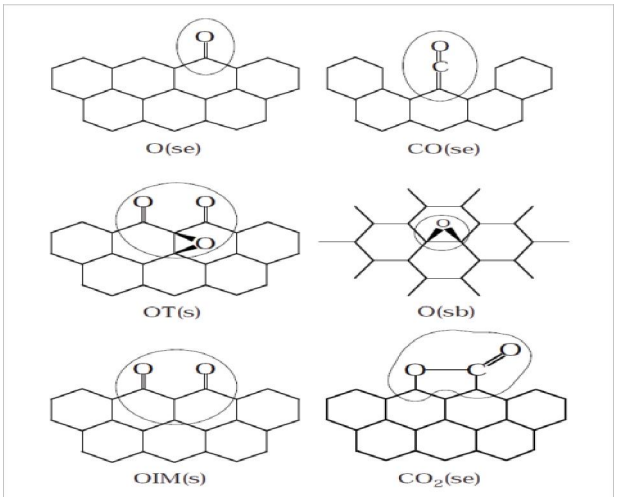

Fig. 6. Scheme of surface complexes used in [14].

This mechanism includes not only oxygen active surface complexes, but also C'(H), C'(OH) and C'($H0_2$). Coefficients of reaction rates have been adopted from literature.

The overall oxidation process of carbon includes chemical reactions and transport within the pore structure [38-39]. Because a theoretical model of the combustion of a porous carbon particle has to include the kinetics of the chemical reactions of carbon with oxygen as an essential part of the model, and the kinetics of this reaction are not sufficiently known at this time, no model of porous carbon combustion exists that describes all features of this process. Only a handful of investigations have considered full transport and reaction within the pores, however with highly simplified heterogeneous and homogeneous kinetic models [40-43]. The developed in [40] model for the combustion of a porous carbon particle considers the equations of heat and mass transfer, both in the gas phase around the particle and inside the pores.

Four chemical reactions have been considered:

$$C + O_2 \rightarrow CO_2$$
$$2C + O_2 \rightarrow 2CO$$
$$C + CO_2 \rightarrow 2CO$$
$$2CO + O_2 = 2CO_2$$

The first three reactions are heterogeneous and can take place either inside a porous particle or at the particle's surface. The last reaction is homogeneous and can occur both in the gas phase near a particle and inside the porous particle. The kinetics of the homogeneous chemical reaction has been adopted from the literature. Two regimes of particle combustion have been analyzed: 1) the regime when carbon reacts with oxygen in the all volume of the particle, and 2) the regime with carbon reacting with

oxygen in a layer at the particle's exterior. Both carbon monoxide and carbon dioxide can be formed in the first regime, but carbon monoxide can only be formed in the second regime.

A general mathematical formulation and a numerical solution approach are developed in [43] to model the oxidation of an isolated porous carbon particle in a quiescent atmosphere under quasi-steady conditions Fig. 7. The gas-phase reaction mechanism proposed by Yetter et al. [44], consisting of 12 species in 28 elementary reactions, was used for modelling CO oxidation. The surface reaction mechanism of Makino et al. [45] for porous carbon was employed first to obtain an initial approximate solution of the gas-phase flame structure. With this initial solution of the gas-phase, the heterogeneous reactions were described with the semi - global surface reaction mechanism of Bradley et al. [46] for non-porous carbon. It should be pointed out that the detailed gas-phase reactions were applied not only to the reactions outside the particle, but also the gaseous reactions within the pore structure. The existence of limiting combustion regime as a function of particle size, porosity, and ambient oxygen mole fraction is explored based on the model developed. Comparison of the predicted particle mass burning rate and surface temperature with recent experiments are in reasonable sufficient agreement.

**Table 3**

The reaction model developed in [14]. Coefficient of reaction rate is $k_j = A_j * exp\ (-E/R*T) * T^{\beta}$, the units of preexponential factor $A_i$ are: [cm, mol, sec], activation energy $E_a$–kJ/mole. $E_a^1 = (28 + 146\Theta_{o(se)})$, $E_a^3 = (358 - 1146\Theta_{o(se)})$, $E_a^{23} = (9 + 280\Theta_{o(se)})$, Θ is the fraction of surface area, occupied with (se)

| # | Reaction | | | A | β | Ea |
|---|---|---|---|---|---|---|
| 1. | $O_2$ + 2 (se) | → | 2 O (se) | 3.1 E16 | 1 | $E_a^1$ |
| 2. | 2 O (se) | → | 2 (se) | 3.7 E21 | 0 | 602 |
| 3. | O (se) | → | CO + (se) | 2.5 E15 | 0 | $E_a^3$ |
| 4. | CO + (se) | → | O (se) | 8.3 E07 | 0 | 162 |
| 5. | $O_2$ + 4 (sb) | → | 2 O (sb) | 4.3 E35 | 1 | 116 |
| 6. | 2 O (sb) | → | $O_2$ + 4 (sb) | 6.0 E19 | 0 | 322 |
| 7. | 2 O (se) + 2 (sb) | → | OIM | 5.0 E38 | 0 | 0 |
| 8. | OIM (s) | → | 2 O (se) + 2 (sb) | 1.0 E13 | 0 | 100 |
| 9. | $O_2$ + OIM (s) + 2 (sb) | → | OT (s) + O (sb) | 4.4 E25 | 1 | 20 |
| 10. | OT (s) + O (sb) | → | $O_2$ + OIM (s) + 2 (sb) | 3.7 E21 | 0 | 107 |
| 11. | OT (s) | → | 2 CO + 2 (sb) + (se) + CO( se) | 1.0 E16 | 0 | 266 |
| 12. | 2 CO + CO (se) + (se) + 2 (sb) | → | OT (s) | 1.0 E20 | 0 | 100 |
| 13. | O (sb) + (se) | → | O (se) + 2 (sb) | 6.0 E19 | 2 | 46 |
| 14. | O (se) + 2 (sb) | → | O (sb) + (se) | 1.4 E30 | 0 | 373 |
| 15. | CO + (se) | → | CO (se) | 6.0 E07 | 0 | 59 |
| 16. | CO (se) | → | CO + (se) | 1.0 E16 | 0 | 145 |
| 17. | O + (se) | → | O (se) | $S_0$ 1.0 | | |
| 18. | O (se) | → | O + (se) | 1.0 E13 | 0 | 500 |
| 19. | O + 2 (sb) | → | O (sb) | $S_0$ 1.0 | | |
| 20. | O (sb) | → | O + 2 (sb) | 1.0 E13 | 0 | 103 |
| 21. | $CO_2$ (se) | → | CO (se) + O (se) | 1.0 E16 | 0 | 267 |
| 22. | CO (se) + O (se) | → | $CO_2$ (se) | 3.7 E21 | 0 | 1 |
| 23. | $CO_2$ (se) + 2 (se) | → | $CO_2$ (se) | 3.1 E16 | 0 | $E_a^{23}$ |
| 24. | $CO_2$ (se) | → | $CO_2$ (se) + 2 (se) | 1.0 E16 | 0 | 468 |
| 25. | O (se) + O (sb) | → | $CO_2$ + (se) + 2 (sb) | 4.8 E20 | 0 | 122 |
| 26. | $CO_2$ + (se) + 2 (sb) | → | O (se) + O (sb) | 1.1 E25 | 1 | 163 |
| 27. | CO + O + M' | ↔ | $CO_2$ + M' | 7.1 E13 | 0 | 19 |
| 28. | CO + $O_2$ | ↔ | $CO_2$ + O | 2.5 E12 | 0 | 200 |
| 29. | C + $O_2$ | ↔ | CO + O | 5.0 E13 | 0 | 0 |

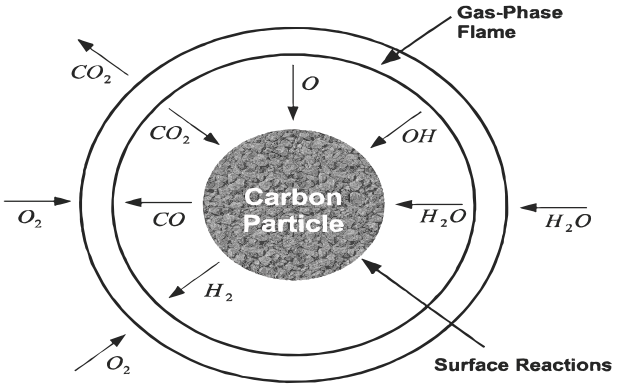


Fig. 7. Illustration to modeling the oxidation of an isolated porous carbon particle in [43].

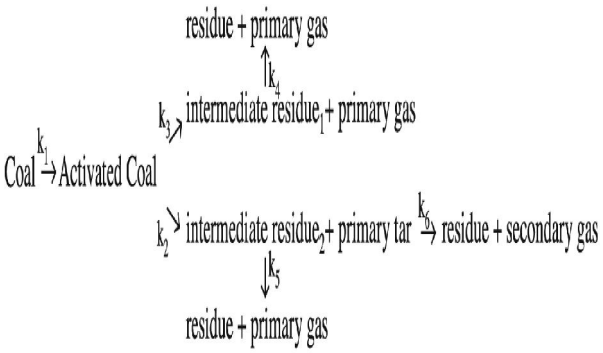


Fig. 8. Main steps of sectional model describing the partially parallel processes at the coal pyrolysis [53].

The next critical point in coal gasification is reactions in surrounding gas. The gas phase chemical kinetics compared to heterogeneous one is based on the comprehensive well validated thermo kinetic properties and is well established especially for small hydrocarbons [47-49]. There are among of reaction mechanisms, which allow successfully modeling of the hydrocarbon oxidation with formation of polycyclic aromatic hydrocarbons (PAHs). The possible PAH formation in coal combustion is demonstrated, for example, in measurements [50]. The PAH measurements were performed at different ambient atmosphere, air temperatures and oxygen concentration. It has been shown that the maximum PAH production appeared at 600 °C for pyrolysis and at 800 °C for combustion conditions. With increasing oxygen concentration, PAH formation from coal combustion decreased significantly. By a coal pyrolysis and acetylene production, in systems with reach content of $C_2H_2$, $C_2H_4$ and benzol molecules, the formation of PAHs and soot is the integral part of the kinetic modeling.

Obviously, despite of notable results obtained in the coal surface reaction modeling, the development of elementary surface reaction models is in primitive stages when compared with counterpart homogeneous reaction models. Considerable uncertainties still exist on the reported kinetic data.

Recently, the sectional modeling approach is used to describe the coal decomposition processes [51-53]. This approach is a reasonable compromise between accuracy and detail of the obtained results and computational efforts, in terms of number of reference species and lumped reactions. The sectional method divides for example the particle mass range into classes of species and describes the particulate decomposition/formation with partially parallel processes, Fig. 8 [53].

A multi-step kinetic model of coal devolatilization proposed in starts from the idea, that coal is constituted by several chemical species evolving independently, according to different kinetics.

The coal devolatilization model discussed in work [53] simply refers to the elemental analysis of the coal, in the usual form C, H, O, S, N and ashes. Composition of several coals of practical interest has been investigated in systematized relatively the content of main components, Fig. 9. The C/H plot of Fig. 9 is thus divided in three triangles, and each coal lies inside one of them. Any individual coal is then considered as a simple linear combination of the three closest reference coals, and its devolatilization is assumed a straightforward weighted combination of the pyrolysis of the reference coals. On this way, all the coals investigated in [53], Fig. 9, have been included in a triangle whose vertexes are pure carbon (CHARC), and two reference coals: a lignite with high oxygen content (COAL_3) and a reference coal without oxygen and particularly rich in hydrogen (COAL_1). A third reference coal (COAL_2) has been selected in the middle of in this triangle, close to a great number of bituminous coals.

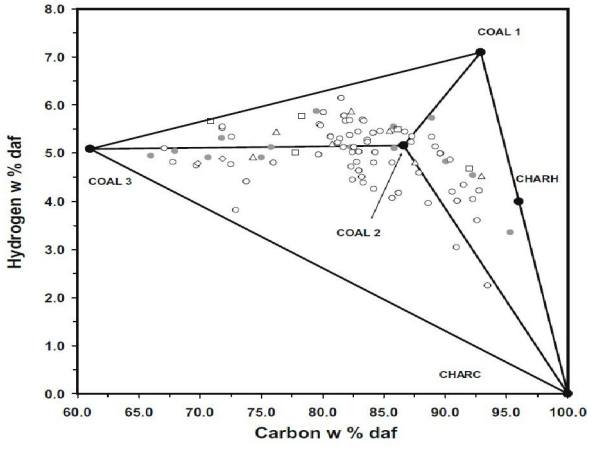


Fig. 9. Composition of investigated coals and reference coal component [53].

These reference coals have been described by three lumped or equivalent monomer structures which stand for reference configurations, saving the elemental C/H/O composition. Figure 10 sketches the average structures of the reference monomers which represents COAL_1 ($–C_{12}H_{11}–$), COAL_2 ($–C_{14}H_{10}O–$) and COAL_3 ($–C_{12}H_{12}O_5–$), respectively. COAL_1 was indeed considered as a 50/50 mol mixture of ($–C_{12}H_{10}–$) and ($–C_{12}H_{12}–$).

A multi-step devolatilization mechanism has been developed to describe the pyrolysis of these reference coals.

The complete reaction scheme, with lumped stoichiometries and all the kinetic parameters, is reported in Table 4 (units are: cal, mol, l, s,). Initially the coal forms a metaplastic phase, then, with different mechanisms at low and high temperatures, gas and tar species are released. The novelty of this kinetic model lies in its predictive approach, without tuning activity of rate parameters and/or stoichiometry for the different coals. Of course, the detail of intermediate species, as well as the number of reference coals, can be modified according to the purpose of the devolatilization model.

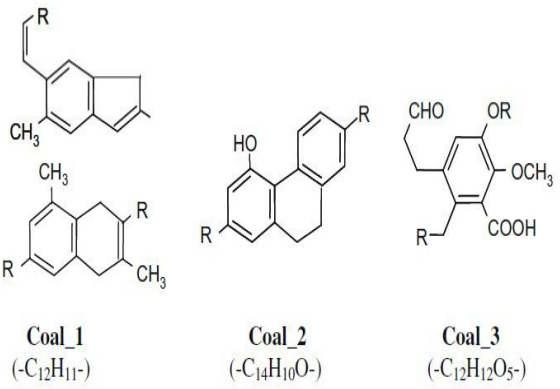


Fig. 10. Reference coals and reference monomer structures [53].

**Table 4**

Multi-step-kinetic model of coal devolatilization [53]

| | | $A^a$ | $E_{ATT}{}^a$ |
|---|---|---|---|
| | ***COAL$_1$(-C$_{12}$H$_{12}$-)*** | | |
| 1. | $COAL_1 \rightarrow 5CHAR_H + .1CHAR_c + 2H_2 + .9CH_4 + 1C^*_{2\text{-}5}$ | $2.0\times10^8$ | 40.000 |
| 2. | $COAL_1 \rightarrow TAR_1^*$ | $1.0\times10^8$ | 40.000 |
| 3. | $COAL_1 \rightarrow 5CHAR_H + .25CHAR_C + .5H_2 + .75CH_4 + 1C_{2\text{-}5}$ | $1.0\times10^{14}$ | 75.000 |
| 4. | $COAL_1 \rightarrow TAR_1^*$ | $1.0\times10^{14}$ | 75.000 |
| 5. | $TAR_1^* \rightarrow TAR_1$ | $2.5\times10^{12}$ | 50.000 |
| 6. | $TAR_1^* + CHAR_H \rightarrow 5.3CHAR_H + 3CHAR_C + 2.55H_2 + .4CH_4$ | $2.5\times10^7$ | 32.500 |
| 7. | $TAR_1^* + CHAR_C \rightarrow 4.3CHAR_H + 4CHAR_C + 2.55H_2 + .4CH_4$ | $2.5\times10^7$ | 32.500 |
| | ***COAL$_2$ (-C$_{14}$H$_{10}$O-)*** | | |
| 8. | $COAL_2 \rightarrow 2CHAR_C + 3.94CHAR_H + .25COAL_1 + .04BTX^* + .31CH_4{}^* + .11C^*_{2\text{-}5} +$ $+ .11\{COH_2\}^* + .15CO_2{}^* + .41H_2O^* + .18CO^* + .265H_2$ | $6.0\times10^{10}$ | 36.000 |
| 9. | $COAL_2 \rightarrow 0.61CHAR_C + 4.33CHAR_H + .21COAL_1 + 16BTX^* + .27CH_4 + 7CO +$ $+ .1H_2O + .2\ \{COH_2\}^* + .28H_2$ | $4.0\times10^{18}$ | 63.000 |
| 10. | $COAL_2 \rightarrow TAR_2^*$ | $5.0\times10^{10}$ | 36.000 |
| 11. | $COAL_2 \rightarrow TAR_2$ | $4.0\times10^{17}$ | 63.000 |
| 12. | $TAR_2^* \rightarrow TAR_2$ | $2.4\times10^9$ | 39.000 |
| 13. | $TAR_2{}^* + CHAR_H \rightarrow 1.5CHAR_C + 7CHAR_H + 1H_2O^* + .5CH_4$ | $4.5\times10^9$ | 30.000 |
| | ***COAL$_3$(-C$_{12}$H$_{12}$O$_5$-)*** | | |
| 14. | $COAL_3 \rightarrow 2.73CHAR_C + 1.8CHAR_H + .22COAL_1 + .08BTX^* + .20_x\text{-}C +$ $+.1CH_4{}^* + .11C^*_{2\text{-}5} + .2H_2O^* + 6(COH_2)^* + 2.2H_2O^* + .1CO_2 + 4CO_2{}^* + 1CO^*$ | $2.0\times10^{10}$ | 33.000 |
| 15. | $COAL_3 \rightarrow COAL_3{}^*$ | $5.0\times10^{18}$ | 61.000 |
| 16. | $COAL_3{}^* \rightarrow 1.5CHAR_H + .82CHAR_c + 2.08CO + .250_x\text{-}C + .14CH_4 + .7C_{2\text{-}5} +$ $+ .5CO_2 + .47\{COH_2\}^* + .16BTX^* + .25COAL_1 + 1.2H_2O + .29H_2$ | $1.2\times10^8$ | 30.000 |
| 17. | $COAL_3 \rightarrow TAR_3{}^* + CO_2{}^* + H_2O$ | $1.6\times10^9$ | 33.000 |
| 18. | $COAL_3 \rightarrow TAR_3 + CO_2 + H_2O$ | $2.0\times10^{18}$ | 61.000 |
| 19. | $TAR_3{}^* + TAR_3$ | $5.0\times10^9$ | 32.500 |
| 20. | $TAR_3{}^*\ CHAR_H \rightarrow 4CHAR_H + 2.5CHAR_C + .2CH_4{}^* + 2\ \{COH_2\}^* + .8H_2 + .3C_{2\text{-}5}$ | $1.4\times10^8$ | 30.000 |

[a] $k = A \exp(-E_{ATT}/RT)$ (units are cal, mol, l, K, and s)

### *Plasma-Assisted Coal Gasification*

Plasma particles are not long-living ions, radicals and exited molecules, therefore the quasi-state assumption cannot be applied if we want to investigate the intrinsic plasma chemistry reactions. To decouple the physical and chemical effects and to investigate the influence of plasma particles on the process, more detailed char surface reaction models are required.

Plasma is a partially or wholly ionized quasi-neutral gas, in which a system contains free positive (ions) and negative (electrons and, rarely, ions) particles so that their concentrations on the whole are practically equal. The source of plasma is usually gas discharge, i.e. plasma is an ionized gas resulting from an electrical discharge. For simplicity, an electric discharge can be viewed as two electrodes inserted into a glass tube and connected to a power supply. Thermal arcs usually carry large currents, greater than 1 A at voltages in the order of tens of volts. Furthermore, they release large amounts of thermal energy at very high temperatures often exceeding 10.000 K. The arcs are often combined with a gas flow to form high-temperature plasma jets.

The basic theoretical principles, overviews devoted to plasma experimental and numerical studies, and plasma practical applications can be found in [54-77].

Temperature is important characteristic of plasma, which determines the type of plasma and consequently the basic properties of plasma gas. In the literature one can meet the terms “high temperature plasma”, plasma with the temperature of heavy particles $T > 10^5$ K and “low temperature plasma” with $T \leq 10^5$ K [55]. Temperature in plasma is determined by the average energies of the plasma particles (neutral and charged) and their relevant degrees of freedom (translational, rotational, vibrational, and those related to electronic excitation). Thus, plasmas, as multi-component systems, are able to exhibit multiple temperatures and non-equlibrium velocity distribution for all types of particles. In such case plasma is called non-equilibrium or non-thermal plasma and is able to operate effectively at low temperatures and pressure.

If the temperatures of electrons and heavy particles approach each other or, in other words, the velocity distribution functions for all types of particles can be assumed as Maxwellian, plasma comes to local thermodynamic equilibrium (or quasi-equilibrium) and can be characterized by single temperature. In this case it is called thermal or equilibrium plasma. Thermal plasma enables the delivery of high power at high operating pressure, generally gas temperature is ≥ 1000 K.

Chemical phenomena in behavior of plasma systems are determined by types of produced active molecules and time scales of elementary “physical & chemical processes”. These strongly depend on the kind of applied gas discharge physics [56-59].

The main types of discharges used to produce thermal plasma are electric (DC/AC Electric Arc Discharge), microwave (MW), radio frequency (RF), etc.; for non-thermal plasma - DBD (dielectric barrier discharge), pulsed MW, pulsed corona and electron beam, etc. [56, 57].

This short information concerning types of plasma is integrated in Table 5.

**Table 5**
Classification of plasma [59, 62]

| Plasma | Parameters | Supplies |
|---|---|---|
| High temperature plasma (equilibrium plasma) | $T_c = T_i = T_n$, $T_p = 10^6\ K$ - $10^8\ K$, $n_c \geq 10^{20}\ m^{-3}$ | Laser fusion plasma, DC/AC arc |
| Low temperature plasma | | |
| Thermal plasma (Quasi-equilibrium plasma) | $T_c \approx T_i \approx T_n$, $T_p = 10^3\ K$ - $10^4\ K$, $n_c \geq 10^{20}\ m^{-3}$ | DC/AC arc microwave, RF |
| Non-thermal plasma (Non-equilibrium plasma) | $T_c \geq T_i \approx T_n$, $T_p = 3 \cdot 10^3\ K$ - $4 \cdot 10^4\ K$, $n_e \geq 10^{10}\ m^{-3}$ | DBD pulsed MW pulsed corona electron beam |

$T_c$ = electron temperature; $T_i$ = ion temperature; $T_n$ = neutral molecul temperature; $T_p$ = plasma temperature; $n_e$ = electron density.

Chemically active plasma is a multi-component system which is highly reactive due to large concentrations of charged particles (electrons, negative and positive ions), excited atoms and molecules (electronic and vibrational excitation being the major contribution), active atoms and radicals, and UV photons. Each component of the chemically active plasma plays its own specific role in plasma-chemical kinetics. Electrons are usually first to receive the energy from an electric field and then distribute it among other plasma components and specific degrees of freedom of the system. Changing parameters of the electron gas (density, electron energy distribution function) often permits to control and optimize plasma-chemical processes. Ions are charged heavy particles, that are able to make a significant contribution to plasma-chemical kinetics either due to their high energy (as in the case of sput-

tering and reactive ion etching) or due to their ability to suppress activation barriers of chemical reactions. This second feature of plasma ions results in the so-called ion or plasma catalysis, which is particularly important in plasma-assisted ignition and flame stabilization, fuel conversion, hydrogen production and exhaust gas cleaning.

The kinetics of equilibrium or quasi-equilibrium plasma-chemical processes is a particular case of non-equilibrium chemical kinetics [55].

Processes in two phase flow, discussed in previous section (heating the coal powder particles, evaporation of volatile material and coal pyrolysis, heterogeneous/porous reactions between char and gas phase environment, chemical reactions in gas phase), Fig. 2, will be now influenced with plasma. With other words, chemical reaction models used in the coal gasification have to include plasma particles and reactions in compliance with properties of applied plasma.

As the plasma flow behavior can be considered fluidic, classical Navier-Stokes equations, equations of continuity, conservation of energy (with plasma heating of particles) and mass of the individual components [5, 7, 15-20] can be applied to model the turbulent two phase plasma jets. But, the Damköhler criterion. $D_a = \tau_l/\tau_c$, ($\tau_l, \tau_c$ are characteristic times of turbulent mixing and chemical reactions) for the majority of the plasma chemical processes at the atmospherical pressure relate to case $D_a \sim 1$, hence, the effect of turbulence on the kinetics of chemical reactions must be taking in consideration, because equality of process scales.

Thus, the plasma assisted coal conversion modeling differs from simulation of an ordinary gasification mostly through the plasma chemical reaction system: interaction between turbulence and chemistry, high temperature reactions, production of active particles and specific plasma reactions must be investigated carefully to understand the influence of plasma on the process. Both, high temperature and high speed of particle heating result in volatile and coal destructing products, which will different from those in low temperature gasification ($T \leq 1200$ K). Heavy aromatic molecules and fragments of tars can be presented in large amounts in the gas phase on the early stage of process. The volatiles initially will react with highly reactive plasma species in very fast reactions to form low molecular gases. High temperature surface and gas phase reactions will dominate in a system.

Specific plasma chemistry reactions require initially to calculate elementary processes and then determine the energy distribution function of particles and to use this information for calculation of process macroscopic parameters.

Main types of plasma chemical reactions are [60]:

molecule dissociation through interactions with plasma electrons

$$e + CH_4 = CH_3 + H + e$$

ionization

$$N(^2P) + O \rightarrow NO^+ + e$$

positive ion and electron recombination

$$O^+ + e + e \rightarrow O + e$$

reaction between neutral components and ions

$$O^+ + O_2 \rightarrow O + O^{+2} + e$$

electron attachment/detachment

$$O + O + e \rightarrow O + O^-$$

$$O + O^- \rightarrow O_2 + e$$

positive ion and electron recombination

$$O^{+2} + e \rightarrow {}^{O+} + O$$

reactions with excited components

$$O + O_2(a\ ^1g) \rightarrow O + O_2$$

The effect of the conditions of the plasma treatment on the chemical and phase compositions, as well as the microstructure and shape of particles can be demonstrated with results obtained in experimental investigations [64]. In this work the influence of three types of gas plasma (1) Ar; (2) Ar + $O_2$ and (3) Ar + $H_2O$ on the coal particle gasification under atmospheric pressure has been performed. The experimental installation used in [64] is shown in Fig. 11.

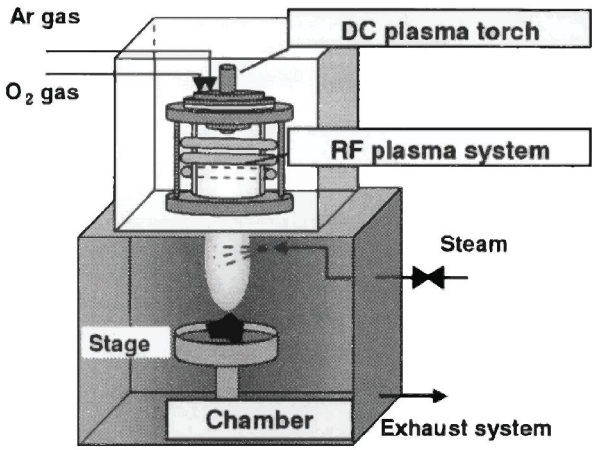


Fig. 11. Experimental installation [64].

One of the main results obtained in [64], is demonstrated in Fig. 12. It can be seen, that in the Ar thermal plasma the fibers of char coal almost retained their shape. In Ar + $O_2$ thermal plasma the fibers of char coal broke up completely. In Ar + $H_2O$ thermal plasma the fibers of the char coal collapsed and looked like melting. Weight of particles, concentrations of CH and $H_2$ were measured after plasma treatment as well. The minimal particle weight reduction, 3.27 g, was detected in the Ar

plasma, the maximal one, 5.92 g, for the Ar + $O_2$ system. Concentrations of CH and $H_2$ over 3 experiments were distributed consequently as 8, 12, 14 ppm and 280, 10, 3300 ppm. The authors concluded that difference reactions occurred on each char coal surface depending on each thermal plasma types.

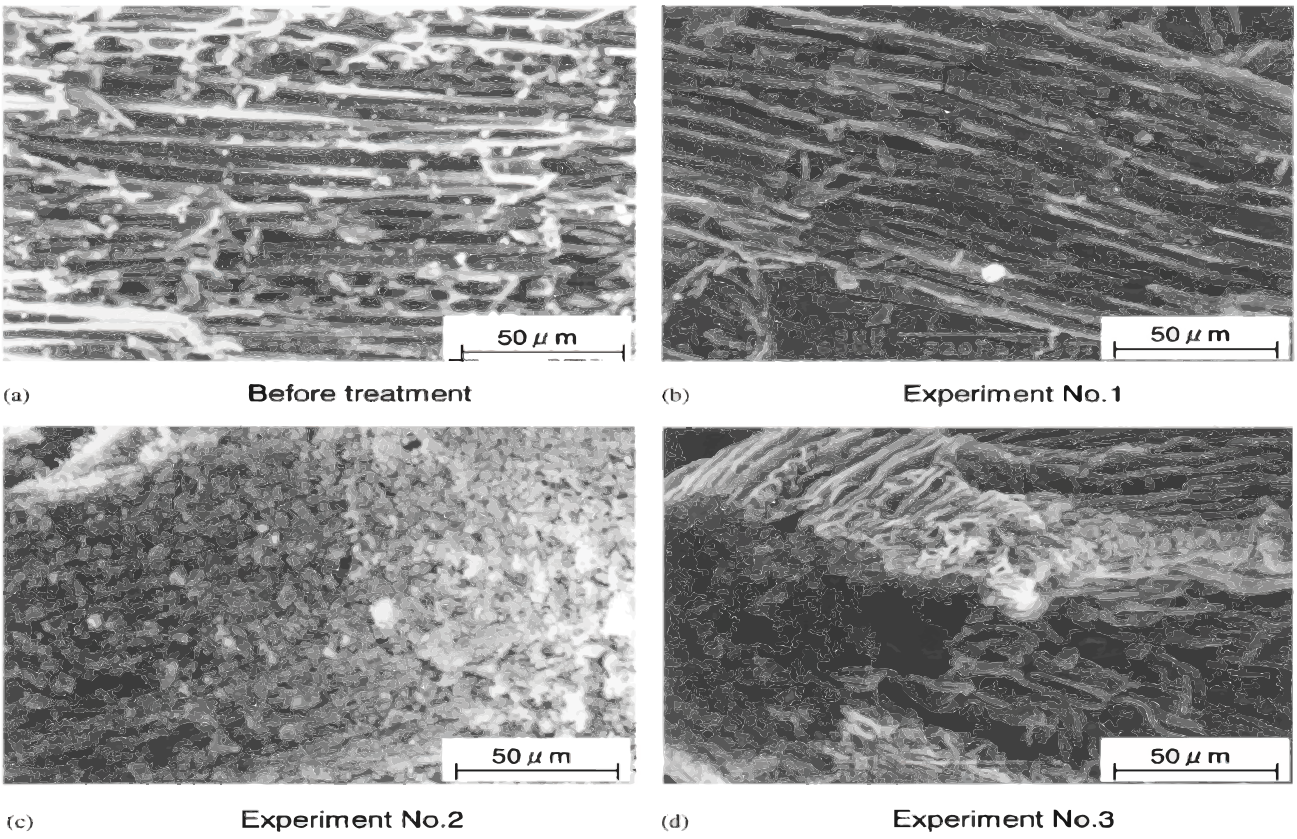


Fig. 12. Micrograph of char coal surface (a) before and after treatment by (b) Ar (c) Ar + $O_2$ (d) Ar + $H_2O$ thermal plasma [64].

In works [1, 2, 19, 65] the results of technology development for plasma assisted coal combustion are presented. Generally, coal-fired utility boilers face two problems, the first being the necessity to use expensive oil for start-up and the second being the increased commercial pressure requiring operators to burn a broader range of coals, possibly outside the specifications envisaged by the manufacturer's assurances for the combustion equipment. The developed technology addressed the above problems is thermochemical plasma preparation of coals for burning.

The plasma-fuel system (PFS) is a cylinder with the plasma generator placed on the burner [1, 2, 19, 65], Fig. 13. In PFS, since the primary mixture is deficient in oxygen, the carbon is oxidised mainly to carbon monoxide.

The air plasma flame is a source of heat and additional oxidation, it provides a high-temperature medium enriched with radicals, where the fuel mixture is heated, volatile components of coal arc extracted, and carbon is partially gasified. This active blended fuel can ignite the main *pf* flow supplied into the furnace. As a result, at the exit from the PFS a highly reactive mixture is formed of combustible gases and partially burned char particles, together with products of combustion, while the temperature of the gaseous mixture is around 1300 K.

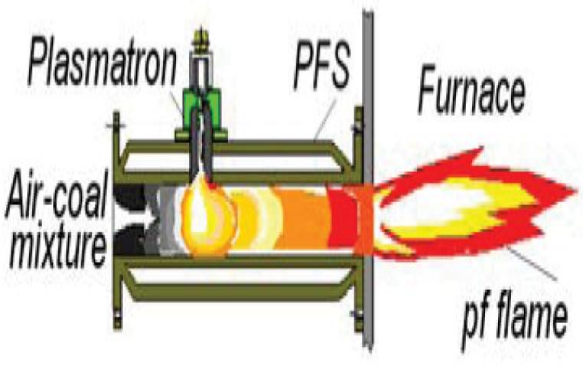


Fig. 13. Plasma-fuel system [65].

Further mixing with the secondary air, upon the introduction of the mixture into the furnace, promotes intensive ignition and complete combustion of the prepared fuel. This technology provides boiler start-up and stabilization of *pf* flame and eliminates the necessity for additional highly reacting fuel. Developed, investigated and industrially tested plasma-fuel systems improve coal combustion efficiency, while decreasing harmful emission from pulverised-coal-fired thermal power plants. From the available experimental data of the PFS operation, the measured composition of the gas phase at the exit of the PFS was (volume %): CO = 28.5; $H_2$ = 8.0; $CH_4$ = 1.5; $CO_2$ = 2.0; $N_2$ = 59.5; $O_2$= 0.0; others = 0.5, including $NO_X$ = 50 mg/nm$^3$.

One-dimensional CFD modelling of FPS [65] with detailed chemical mechanism shown in Table 2, has been carried out in [2]. The reacting flow in the PFS (coal particles/gas mixture) with an internal heat source (electric arc or plasma flame) and thermochemical transformations is formulated within the framework of a one-dimensional plug flow reactor. The heat and momentum exchange, as well as the particle-to-particle, gas-to-particle and gas-to-electric arc heat and mass exchange are accounted for in this model. The fuel chemical transformations considered in this model are as follows: devolatilisation, gasification of char carbon and conversion of evolved volatile products in the gas phase. The arc was taken into account in the balance of energy as an internal source of heat present along the axis of the PFS, the strength of the heat source being ascribed from the experiment data. The computational procedure was subdivided into two stages. The first stage included the computation of the heating of the coal/air mixture by the plasma flame to a temperature corresponding to the onset of devolatilisation, the ignition of the volatiles, and the gasification of the char. Then the plasma heat source is deactivated and computation of all thermo-chemical and gasification processes is continued along with the computation of the one-dimensional two phase (gas plus particles) fluid mechanics. 3D computation for the real PFS geometry has been performed with assummsion that reactions are fast and in equilibrium. The equilibrium chemistry solution procedure is performed using the numerical approach TERRA [19]. Intrinsic plasma chemistry reactions have been not used in modelling [2, 19].

Plasma - steam gasification of petrocoke has been studied in [66]. Petrocoke is solid fuel consisted of fixed carbon, tar, and ash. Direct utilization of the petrocoke is difficult because of its low mechanical hardness and high tar content. A potential method to use petrocoke is steam gasification that converts the organic mass of the coke into high-calorific synthesis gas (CO + $H_2$) that is free from nitrogen and sulphur oxides in the plasma reactor.

This conversion can be written as:

$$C + H_2O = CO + H_2 - Q = 131500 \text{ kJ/mol}.$$

The plasma source energy compensates the heat was varied from 3 to 3.5 kg/h. The plasma reactor power was 60 kW. 2500 K mass averaged temperature in the reactor was achieved. The coke gasification degree was 76.3 to 78.6%. The composition of the gas phase was (vol.%) $H_2$, 53.5 to 57.4%, CO, 33.9 to 36.2%, $N_2$, 6.0 to 11.8%, $O_2$, 0.4 to 0.8%.

The gasification of coal under steam and air plasma conditions at atmospheric pressure was investigated in [67] in a tube-type setup with an aim of producing the synthesis gas. The different factors influence the process have been analysed carefully. The plasma was diagnosed by optical emission spectroscopy and the synthesis gas was analyzed by gas chromatography. It has been found that the content of $H_2$ and CO in gas increases with increasing the arc input power, and passes through a maximum with the increase of current in electromagnetic coil, while the content of $CO_2$ and $O_2$ in the gas decreases. The content of $H_2$ + CO in the gas reaches 75 vol.% when the arc input power is 72.5 kW, while the content of $CO_2$ remains to be less than 3 vol.%. Obviously, high input power favours the formation of $H_2$ and CO, but it should be noted that the content of $H_2$ and CO in gas increases slightly with further increasing the arc input power. This implies that it will not be economical to further increase the arc input power unlimitedly.

It has been establish that the intensity of the emission peaks of $CO^+$ ion and CH radical in the plasma increases roughly with increasing the arc input power and correlate with CO and $H_2$ concentrations. This strongly implies that the $CO^+$ ion and CH radical are the precursors or origins of CO and $H_2$ in the final gas products. The process parameters including the arc input power, the electromagnetic coil current and the coal-feeding rate have an important effect on the gas composition.

The plasma applications for coal pyrolysis, acetylene production, non-nuclear waste pyrolysis can be recognized in [62, 68-71].

All described investigations present the results of phenomenological studies of processes. Unfortunately, the kinetic modelling of plasma chemistry in coal gasification has been not found in open literature. One can say that a physicochemical kinetic mechanism applied to plasma gasification modeling, i.e. the determination and description of the

necessary set of plasma chemistry substances and heterogeneous/homogeneous reactions is not developed today.

On the other side, considerable progress has been made recently in experimental and numerical investigation of plasma-assisted hydrocarbon combustion [56-61, 72-77], with development of detailed reaction mechanisms for the plasma assisted hydrocarbon oxidation.

Transient plasma induced production of OH [68] is followed in a quiescent, stoichiometric $CH_4$–air mixture using the planar laser induced fluorescence technique. Ignition and subsequent flame propagation, for both the transient plasma and traditional spark ignition, are observed. The transient plasma is generated using a 70 ns FWHM, 60 kV, 800 mJ pulse. OH production was confirmed throughout the chamber volume. Ignition induced by transient plasma was decidedly faster than by spark ignition. Analysis of the flame front propagation rates shows that flames ignited by transient plasma propagate essentially at the speed consistent with well accepted literature values for the stoichiometric methane–air mixture. This supports the notion that residue plasma, if any, has little effect on flame propagation. Water vapor in the mixture gives several important pathways for streamer-induced OH production: direct electron impact disassociation of water vapor and the creation of $O(^1D)$, which reacts with water vapor to produce OH:

$$e + H_2O \rightarrow H + OH + e,$$
$$e + O_2 \rightarrow O(^1D) + O + e,$$
$$O(^1D) + H_2O \rightarrow 2OH.$$

Kinetic schemes to simulate the production of active particles during the discharge and in its afterglow and then plasma-assisted combustion for $H_2$, $CH_4$, $C_2H_6$ were developed in [61, 63, 73-75]. These works establish the main principals of the plasma-assisted ignition modelling and investigate properties of hydrocarbon combustion with the plasma applying.

In [61] oxidation of molecular hydrogen in a stoichiometric hydrogen–air mixture in the fast ionization wave (FIW) was studied at total pressures $p$ = 1-8 Torr, and the detailed kinetics of the process has been numerically investigated. In this work during the modelling of chemical reactions in the $H_2$–$O_2$–$N_2$ system level-to-level kinetics of the exchange of vibrational energy between $H_2$, $O_2$, $N_2$, OH and $H_2O$ have been taken into account. It was suggested that the behaviour of electron energy distribution function (EEDF) and, respectively, rates of all the processes with participation of electrons are determined by e, $N_2$, $O_2$, $H_2$ and $H_2O$. The list of processes that are allowed for in EEDF computation is given. The kinetic scheme that describes processes at the stage of electric current flow consists of ~750 chemical and ~ 8700 vibrational exchange processes with participation of 254 particles including electron-excited and charged atoms and molecules, electrons, radicals, non-excited components, and vibrational-excited molecules $H_2$, $O_2$, $N_2$ and $H_2O$ and the OH-radical. Corresponding kinetic equations were generated automatically. The following processes were taken into account: associative and Penning ionization, recombination of positive ions and electrons, attachment of electrons to atoms, detachment of electrons, interaction between neutral non-excited components, interaction between neutral excited and neutral non-excited components, conversion of positive and negative ions, and recombination of positive and negative ions.

Diagrams of active particle flows were constructed for every time interval for the most rapid channels of chemical conversions. The performed analysis shown that under conditions of pulsed high-voltage breakdown the gas is excited predominantly behind the fast ionization wave front at the stage of quasi-stationary high-current discharge in relatively weak electric fields $E/n$ _ 300-600 *Td* at electron number density $ne = (1\text{-}2) \times 1012\ cm^{-3}$ for a time of the order of 10 *ns*. In the following processes for times up to 100 *ns* the dominant role belongs to reactions with electron excited particles participation; in the microsecond time range it belongs to the ion–molecular reactions; in the time interval of 100 $\mu s$–25 *ms* the main contribution is made by reactions with participation of radicals.

Kosarev et al. in [73] the kinetics of ignition in a $CH_4$:$O_2$:Ar mixture under the action of a high-voltage nanosecond discharge have studied experimentally and numerically. Ignition delay time behind a reflected shock wave was measured with and without the discharge. It was shown that the initiation of the gas discharge with a specific deposited energy of 10-30 $mJ/cm^3$ leads to an orders-of-magnitude decrease in ignition delay time. Discharge processes and following chain chemical reactions with energy release were simulated separately because of an essential difference in their time scales. A kinetic scheme was developed to simulate the production of active particles during the discharge and in its afterglow. The generation of atoms, radicals, and excited and charged particles was numerically simulated using measured time-resolved discharge current and electric field in the discharge phase.

Under the conditions considered, the discharge processes occurred on a nanosecond scale, whereas

the ignition processes occurred on a microsecond scale. Therefore, the temporal evolution of densities of particles important for plasma assisted ignition was simulated separately in the discharge phase and in the ignition phase. The calculated densities of active particles were used as input data to simulate plasma-assisted ignition of methane.

It was assumed that the effect of non-equilibrium discharge plasma is reduced to the accumulation of active particles that influence the ignition processes. The active particles under consideration were electronically excited $O_2$ molecules and Ar atoms, O atoms, H atoms, radicals of hydrocarbon molecules, electrons, and simple positive ions. The focus was on the mechanisms that could lead to dissociation of molecules.

The electron Boltzmann equation was solved numerically in the classical two term approximation to determine the non-equilibrium electron energy distribution. In solving the Boltzmann equation, the input parameters were the reduced electric field *E/n* and gas composition. The electron distribution was not sensitive to gas temperature. Only electron collisions with atoms and molecules of the dominant species in the gas mixture were considered. The effect of electron–electron collisions and collisions between electrons and new particles produced in the discharge was neglected because of the low densities of these particles. For electron collisions with Ar, $O_2$, and $CH_4$, the self-consistent sets of cross sections, available in the literature, were used, which allow good agreement between calculations and measurements of transport and rate coefficients in the pure gases. The reaction rates parameters were taken from the literature or calculated. The ignition process was numerically simulated using the kinetic mechanism RAMEC suggested in [78]. This mechanism is based on the kinetic scheme GRI-Mech 1.2 [79]. The calculated ignition delay time agrees well with experimental data.

In [76] the kinetics of alkane oxidation has been measured from methane to decane in stoichiometric and lean mixtures with oxygen and air at room temperature under the action of high-voltage nanosecond uniform discharge.

The complete self-consistent calculations of the heterogeneous /homogeneous plasma chemical process are at present not possible because of mathematical difficulties and the absence of chemical kinetic and experimental data for modelling. After determination of the region of applicability, i.e. parameters of plasma chemical systems, the most significant characteristics of the process, initial data and target parameters, different simplifications of reaction mechanisms for plasma chemistry can be performed. In [77] of such simplified model for the production of the main species present in the air plasma - $N_2$, $O_2$, N, O, NO (neutral species) and $NO^+$, $N_2$,$^+$ $O_2^+$,$O^+$, e (charged species) has been proposed.

## Conclusions

Coal gasification (partial coal combustion) is a complex process accompanied by two-phase turbulent flow, heat transfer, combustion and gasification.

Mathematical models and CFD tools for coal gasification have been developed, which describe heating, evaporation, pyrolysis of coal and coke particles, the heterogeneous/porous reactions, the gas phase reactions operating very simple empirical chemical sub-models.

Plasma-assisted coal gasification is a possibility to accelerate, manage and optimise the process of coal gasification. Both thermal and non-thermal plasma discharges can be used to convert coal into other fuels. The benefits of plasma application in these technologies can be based on the high selectivity of the plasma-chemical processes, the high efficiency of conversion of different types of coal including those of low quality, relative simplicity of the process control, and significant reduction of ashes, sulphur, and nitrogen oxides output.

The main problems in coal gasification modeling are incomplete initial information on the properties of substances and characteristics of physical and chemical processes as well as the absence of reasonably “efficient” theories of describing the processes. Neither plasma-assisted gas phase reactions nor plasma-assisted heterogeneous reactions of coal gasification are available in the open literature.

But, the progress in theoretical methods, application of state-of-the-art electronic structure methods, theory of elementary processes and in computer science allows us today to generate complete set of data for plasma chemical process simulation.

## References

1. Messerle, V.E. and Peregudov, V.S., 1995, “Ignition and Stabilisation of Combustion of Pulverised Coal Fuels by Thermal Plasma. Investigation and Design of Thermal Plasma Technology”, Cambridge Interscience Publishing, London, 2, pp. 323-343.
2. Gorokhovski, M.A., Jankoski, Z., Lockwood, F. C., Karpenko, E.I., Messerle, V.E. and Ustimenko, A.B., 2007, “Enhancement of pulverized coal combustion by plasma technology”, Combust. Sci. and Technol. 179(10), pp. 2065-2090.

3. Green E.S., Meyreddy R.R., Pamidimukkala K. M., 2008, “A molecular model of coal pyrolysis”, International Journal of Quantum Chemistry 26(S18), pp. 589-599.
4. Zhukov, M.F., Kalinenko, R.A., Levicki, A.A., Polak, L.S., 1990, “Plasmochimichskaya perabotka uglja” (in Russia), Moskva, Nauka, pp. 200.
5. Basic Technologies for Advanced Coal Utilization, NEDO-commissioned project, 2004, FY2000-FY2004, Japan Coal Energy Center.
6. Lemaignen, L., Zhuo, Y., Reed, G.P., Dugwell, D.R., Kandiyoti, R., 2002, “Factors governing reactivity in low temperature coal gasification. Part II. An attempt to correlate conversion with inorganic and mineral constituents”, Fuel 81, pp. 315-325.
7. Liu, G., Benyon P., Benfell, K.E., et al., 2000, “The porous structure of bituminous coal chars and its influence on combustion and gasification under chemically controlled conditions”, Fuel 79 , pp. 617-626.
8. Wall, T.F., Liu, G., Wu, H., Roberts, D., et al., 2002, “The effects of pressure on coal reactions during pulverised coal combustion and gasification“, Prog.Ener.Comb.Sci. 28, pp. 405-433.
9. Niksa, S., Liu, G., Hurt, R. H., 2003, "Coal conversion submodels for design applications at elevated pressures. Part I. devolatilization and char oxidation", Prog. Ener. Comb. Sci. 29, pp. 425-477.
10. Liu, G., Niksa S., 2004, "Coal conversion submodels for design applications at elevated pressures. Part II. Char gasification", Prog. Ener. Comb. Sci. 30, pp. 679-717.
11. Zhuo, Y., Messenböck, R., Collot, A.-G., Megaritis, A., Paterson, N., Dugwell, D.R., Kandiyoti, R. 2000, “Conversion of coal particles in pyrolysis and gasification: comparison of conversions in a pilot-scale gasifier and bench-scale test equipment”, Fuel 79, pp. 793-802.
12. Hurt, R.H., Calo, J.M., “Semi-global intrinsic kinetics for char combustion modeling”, 2001, Combust. Flame 125, pp. 1138-1149.
13. Wang, H., Dlugogorski, B.Z., Kennedy, E.M., “Kinetic Modeling of Low-Temperature Oxidation of Coal”, 2002, Combust. Flame 131, pp. 452-469.
14. Mießen, G., 2000, “Simulation der Koksverbrennung unter Verwendung detaillierter Reaktionsmechanismen”, PhD Dissertation, Ruprecht - Karls – Universität Heidelberg.
15. Gentry, R.A., Daly, B.J. and Amsden, A.A., 1987, KIVACOAL: A modified version of the KIVA program for calculating the combustion dynamics of a coal-water slurry in a diesel engine cylinder, Los Alamos National Laboratory Report LA-l 1045-MS .
16. Radulovic, P.T., Ghani, M.U., Smoot, L.D., 1995, “An improved model for fixed bed coal combustion and gasification”, Fuel 74 , pp. 582-594.
17. Lockwood, F.C., Mahmud, T., and Yehia, M.A., 1998, “Simulation of pulverised coal test furnace performance”, Fuel 77(12), pp. 1329-1337.
18. Yang, L., 2004, “Study on the model experiment and numerical simulation for underground coal gasification”, Fuel 83, pp. 573-584.
19. Gorokhovski, M., Karpenko, E.I., Lockwood, F. C., Messerle, V.E., B. Trusov, G., Ustimenko, A.B., 2005. “Plasma technologies for solid fuels:experiment and theory”, Journal of the Energy Institute 78(4), pp. 157-171.
20. Piffaretti, S., Abdon, A., Engelbrecht, E. G. et al., 2008, “Validation of a cfd based modelling approach to predict coal combustion using detailed measurements within a pulverized coal boiler”, ANSYS Conference & 26. CADFEM users’ meeting, Darmstadt, Germany.
21. Molina, A. and Mondrago, N.F., 1998. “Reactivity of coal gasification with steam and $CO_2$”, Fuel 77(15), pp. 1831-1839.
22. Choi, Y.C., Li, X.Y., Park, T.J., Kim, J.H., Lee, J.G., 2001, “Numerical study on the coal gasification characteristics in an entrained flow gasifier”, Fuel 80, pp. 2193-2201.
23. Biba, V., Macak, J., Klose, E., Malecha, J., 1978, “Mathematical Model for the Gasification of Coal under Pressure”, Ind. Eng. Chem. Process Des. Dev. 17(1), pp. 92-98.
24. Beath, A.C., 1996, “Mathematical modelling of entrained flow coal gasification”, PhD Thesis, University of Newcastle, Australia.
25. Norman, J.J., Pourkashanian, M., Williams, A., 1997, “Modelling the formation and emission of environmentally unfriendly coal species in some”, Fuel 76(13), pp. 201-1216.
26. Kerinin, E.V., Shifrin, E.I., 1993, ”Mathematical model of coal combustion and gasification in a passage on a underground gas generator”, Translation from Fizika Goreniya I vzryva (on Russia), 29(2), pp. 21-28.
27. Kalinenko R.A., Kuznetsov, A.P., Levitsky, A.A., Messerle, V.E., 1993, “Pulverized Coal Plasma gasification”, Plasma Chemistry and Plasma Processing 13(1), pp. 141-167.
28. Kayhan, F., Reklaitis, J.V., 1980, “Modelling of staged fluidized bed coal pyrolysis reactors”, Ind. and Eng.Chem.Process Des. and Develop. 19, pp. 15-23.

29. Kyotani, T., Ito K., Tomita, A., Radovic, L. R., 1996, “Monte Carlo Simulation of Carbon Gasification Using Molecular Orbital Theory”, AIChE Journal 42(8), pp. 2303-2307.
30. Chen, S.G., Yang, R.T., Kapteijn F., Moulijn J.A., 1993, “ A new surface oxygen complex on carbon: toward a unified mechanism for carbon gasification reaction”, Ind.Eng.Che.Res. 32, pp. 2535-2540.
31. Ahmed, S., Back, M.H., Roscoe, J.M., 1987, “A Kinetic Model for the Low Temperature Oxidation of Carbon: I.”, Combust. Flame 70, pp. 1-16.
32. Back, M.H., 1997, “The kinetics of the reaction of carbon with oxygen.”, Can. J. Chem. 75, pp. 249-257.
33. Crick, T.M., Silveston, P.L., Miura, K., Hashimoto, K., 1993, “ Analysis of coal char gasification by use of the pulse method and 18O Isotope”, Energy Fuels 7, pp. 1054-1061.
34. Moulijn, J.A., Kapteijn, F., 1995, “Towards a uni_ed theory of reactions of carbon with oxygen-containig molecules”, Carbon 33(8), pp. 1155-1165.
35. Skokova, K. and Radovic, L.R., 1996, “On the Role of Carbon-Oxygen Surface Complexes in the Carbon/Oxygen Reaction Mechanism,” ACS National Meeting, New Orleans.
36. Radovic, L.R., Quli, F.A., Karra, M., Kokenes, S.C., Skokova, K.A., Lee, Y.-J. and Thrower, P.A., 1997, “Oxidation Resistance of Carbon/ Carbon Composites: Effects of Porosity and Heteroatoms,” International Conference in Commemoration of the 45th Anniversary of Chungnam National University, Taejon, Korea.
37. Mitchell, R.E., Kee, R.J., Glarborg, P., and Coltrin, M.E., 1991, “The effect of CO conversion in the boundary layers surrounding pulverized-coal char particles”, Proc. Combuts. Inst. 23, pp. 1169-1176.
38. Libby, P. A., and Blake, T. R., 1979, “Theoretical study of burning carbon particles”, Combust. Flame 36, pp. 139-169.
39. Smith, I.W., 1982, “The combustion rate of coal chars: a review”, Proc. Combust. Inst. 19, pp. 1045-1065.
40. Gremyachkin, V. M., Förtsch, D., Schnell, U., Hein K.R.G., 2002, ”A Model of the Combustion of a Porous Carbon Particle in Oxygen”, Combust. Flame 130, pp. 161-170.
41. Chelliah, H.K., Makino, A., Kato, I., Araki, N. and Law, C.K., 1996, “Effects of porosity and carbon radical reactions on graphite oxidation”, Combust. Flame 104, pp. 469-480.
42. Murphy, J.J., Shaddix,C. R., 2006, “Combustion kinetics of coal chars in oxygen-enriched environments“, Combust. Flame 144, pp. 710-729.
43. Kassebaum, J.L., Chelliah, H.K., 2009, “Oxidation of isolated porous carbon particles: Comprehensive numerical model”, Combustion Theory and Modelling 13(1), pp. 143-166
44. Yetter, R.A., Dryer, F.L. and Rabitz, H., 1991, “Flow reactor studies of carbon monoxide/ hydrogen/ oxygen kinetics”, Combust. Sci. and Technol. 79, pp. 129-140.
45. Makino, A., Araki, N. and Mihara, Y., 1994, “Combustion of artificial graphite in stagnation flow: Estimation of global kinetic parameters from experimental results”, Combust. Flame 96, pp. 261-274.
46. Bradley, D., Dixon-Lewis, G., Habik, S.E. and Mushi, E.M.J., 1984, “The Oxidation of Graphite Powder in Flame Reaction Zones”, Proc. Combust. Inst. 20, pp. 931-940.
47. Frenklach, M., Wang, H., 1994, “Detailed Mechanism and Modeling of Soot Particle Formation”, ed. H. Bockhorn, Springer-Verlag Berlin, Springer Series in Chemical Physics, 59, p. 165.
48. Konnov, A.A. 2000 “Development and validation of a detailed reaction mechanism for the combustion of small hydrocarbons”, Proc. Combust. Inst. 28, Abstr. Symp. Pap. p. 317.
49. Slavinskaya, N.A., Frank, P., 2009, “A Modeling Study of Aromatic Soot Precursors in Laminar Methane and Ethene Flames”, Combust. Flame 156 pp. 1705-1722.
50. You, X. F., Gorokhovski, M. A., Chinnayya, A., Chtab, A., Cen, K. F., 2007, “Experimental study and global model of PAH formation from coal combustion”, Journal of the Energy Institute 80(1), pp. 12-23.
51. Ranzi E., Cuoci A., Faravelli T., Frassoldati A., Migliavacca G., Pierucci S., Sommariva S., “Chemical Kinetics of Biomass Pyrolysis”, 2008, Energy Fuels, 22, pp. 4292-300.
52. T. Faravelli, A. Frassoldati, G. Migliavacca, E. Ranzi, “Detailed kinetic modeling of the thermal degradation of lignins”, 2010, Biomass and bioenergy 34, pp. 290-301.
53. Sommariva S., Maffei T., Migliavacca G., Faravelli T., Ranzi E., “A predictive multi-step kinetic model of coal devolatilization”, 2010, Fuel 89, pp. 318-328.
54. Bugaenko, L.T., Kuzmin, M.G., Polak, L.S., 1993, “High – Energy Chemistry”, Book craft Ltd, Midsomer Norton, Avon, UK, pp. 404.
55. Polak, L.S., Lebedev, Yu.A. et al., 1998, "Plasma Chemestry", Cambridge International Science Publishing, pp. 390.

56. Fridman, A., Chirokov, A., Gutsol, A., 2005, “Non-thermal atmospheric pressure discharges”, J. Phys. D: Appl. Phys., 38, R1-R24.
57. Starikovskaia, S. M., 2006, “Plasma assisted ignition and combustion”, J. Phys. D: Appl. Phys. 39 , R265-R299.
58. Gleizes, A., Gonzalez J.J., Freton, P., 2005, “Thermal plasma modeling”, J. Phys. D: Appl. Phys. 38, R153–R183.
59. Fridman, A., 2008, “Plasma Chemistry”, Cambridge University Press, New York.
60. Starikovskaia, S. M., Anikin, N. B., Pancheshnyi, S. V., Zatsepin, D. V., Starikovskii, A. Yu., 2001, “Pulsed breakdown at high over voltage: development, propagation and energy branching. Plasma Sources”, Sci. Technol. 10, pp. 344-355.
61. Bozhenkov, S.A., Starikovskaia, S.M., Starikovskii, A.Yu, 2003, “Nanosecond gas discharge ignition of $H_2$- and $CH_4$-containing mixtures”, Combust. Flame 133, pp. 133-146.
62. Babu, B.V., 2007, “Chemical kinetics and dynamics of plasma assisted pyrolysis of assorted, non nuclear waste”. Proceedings of One day discussion meeting on “New Research directions in the use of power beams for environmental applications (RPDM-PBEA-2007)”, Laser & Plasma Technology Division, Bhabha Atomic Research Centre (BARC), Mumbai, September 18.
63. Stariskovskaia, S.M., Starikovskii, A.Yu., Zatsepin, D.V., 2001, “Hydrogen oxidation in stoechiometric hydrogen-air mixture in the fast ionization wave”, Combustion Theory and Modelling 5(1), pp. 97-129.
64. Hiroshi, N., Masaki, I., Tanaka, M. et al., 2004, “A treatment of carbonaceous wastes using thermal plasma with steam”, Vacuum 73, pp. 589-593.
65. Karpenko, E.I., Messerle, V.E., Ustimenko, A.B., 2007, “Plasma-aided solid fuel combustion”, Proc. Combust. Inst. 31, pp. 3353-3360.
66. Lavrichshev, O.A., Messerle, V.E., Osadchaya, E.F., Ustimenko, A.B., 2008, ”Plasma gasification of coal and petrocoke”, 35th EPS Conference on Plasma Phys. Hersonissos, 9-13 June, 2008, ECA Vol.32D, O-2.018.
67. Qiu, J., He, X., Sun, T., Zhao, Z., Zhou, Y., Guo, S., Zhang, J., Ma, T., 2004, “Coal gasification in steam and air medium under plasma conditions: a preliminary study”, Fuel Proc. Technol. 85, pp. 969-982.
68. Chakravartty, S.C., Dutta, D., Lahiri, A., 1975, “Reaction of coals under plasma conditions: direct production of acethylene from coal”, Fuel 55, pp. 43-46.
69. Baumann, H., Bittner, D., Beiers, H.-G., Klein, J., Jüntgen, H., 1988, “Pyrolisys of coal in hydrogen and helium plasma“, Fuel 67, pp. 1120-1123.
70. Bittner, D., Wanzl, W., 1990, “The significance of coal properties for acethylene formation in a hydrogen plasma”, Fuel Proc. Technol. 24, pp. 311-316.
71. Plotsczuk, W.W., Resztak, A., Szymañski, A., 1995, “Plasma processing of brown coal”, Int. J. of Materials and Product Technology 10(3-6), pp. 530-540.
72. Cathey, C., Cain, J., Wang, H., Gundersen, M.A., Carter, C., Ryan, M., 2008, “OH production by transient plasma and mechanism of flame ignition and propagation in quiescent methane–air mixtures”, Combust. Flame 154, pp. 715-727.
73. Kosarev, I.N., Aleksandrov, N.L., Kindysheva, S.V., Starikovskaia, S.M., Starikovskii, A.Yu., 2008, “Kinetics of ignition of saturated hydrocarbons by nonequilibrium plasma: $CH_4$-containing mixtures”, Combust. Flame 154, pp. 569-586.
74. Deminsky, M., Jivotov, V., Potapkin, B., Rusanov, V., 2002, “Plasma-assisted production of hydrogen from hydrocarbons”, Pure Appl. Chem.74(3), pp. 413-418.
75. Deminsky, M., 2009, “Plasma chemical mechanism understanding via partial modeling”, invited lecture, ISPC-19, Bochum, Germany.
76. Starikovskii, A.Yu., Anikin, N. B., Kosarev, I. N., Mintoussov, E. I., Starikovskaia, S. M., Zhukov, V. P., 2006, “Plasma-assisted combustion”, Pure Appl. Chem. 78(6), pp. 1265-1298.
77. Andari, J.AI., Diamy, A.M., Legrand, J.C., Ben-Aim R.I., 1993, “Air Microwave-Induced Plasma: Relation between Ion Density and Atomic Oxygen Density”, Plasma Chemistry and Plasma Processing 13(1), pp. 103-116.
78. Petersen, E.L., Davidson, D.F., Hanson, R.K., 1999, “Kinetics modeling of shock-induced ignition in low-dilution $CH_4/O_2$ mixtures at high pressures and intermediate temperatures”, Combust.Flame 117, pp. 272-290.
79. Frenklach, M., Wang, H., Goldenberg, M., Smith, G.P., Golden, D.M., Bowman, C.T., Hanson, R.K., Gardiner, W.C., Lissianski, V., in: GRI, Topical Report No. GRI-95/0058, 1995.

*Received 20 August 2012*